2-25-2006

Short-pulse laser propagation through tissue medium for tumor detection

Gopalendu Pal

Kunal Mitra

Tuan Vo-Dinh

Short-Pulse Laser Propagation Through Tissue Medium For Tumor Detection

Gopalendu Pal[a], Kunal Mitra*[a], Tuan Vo-Dinh**[b]

[a]Florida Institute of Technology; [b]Oak Ridge National Laboratory

ABSTRACT

The objective of this paper is to perform a comprehensive experimental and numerical analysis of the short pulse laser interaction with tissue medium with the goal of tumor / cancer diagnostics. For short pulse laser source, the shape of output signal is a function of the optical properties of the medium and hence the scattered temporal optical signal helps in understanding of the medium characteristics. Initially experiments are performed on tissue phantoms imbedded with inhomogeneities in order to optimize the time-resolved optical detection scheme. Both the temporal and the spatial profiles of the scattered reflected and transmitted optical signals are compared with the numerical modeling results obtained by solving the transient radiative transport equation using the discrete ordinates technique. Next experiments are performed on *in vitro* rat tissue samples to characterize the interaction of light with skin layers and to validate the time varying optical signatures with the numerical model. The numerical modeling results and the experimental measurements are in excellent agreement for the different parameters studied in this paper. The final step is to perform *in vivo* imaging of anaesthetized rats with tumor-promoting agents injected inside skin tissues in order to demonstrate the feasibility of the technique in detecting tumors in animal model.

Keywords: short pulse laser, imaging, transient radiative transfer, tissues, tumor

1. INTRODUCTION

The use of light for probing and imaging of biological tissue media offers the promise for safe, noninvasive, and inexpensive clinical imaging modalities with diagnostic ability. The detection of early neoplastic changes is important from an outcome viewpoint since once invasive carcinoma and metastases have occurred, treatment is difficult. At present, excisional biopsy followed by histology is considered to be one of the "gold standard" for the diagnosis of early neoplastic changes and carcinoma. In some cases, cytology rather than excisional biopsy is performed. These techniques are powerful diagnostic tools because they provide high-resolution spatial and morphological information of the cellular and subcellular structures of tissues. The use of staining and processing can enhance contrast and specificity of histopathology. However, both of these diagnostic procedures require physical removal of specimens followed by tissue processing in the laboratory. As such, these procedures incur a relatively high cost because specimen handling is required and, more importantly, diagnostic information is not available in real time. Moreover, in the context of detecting early neoplastic changes, both excisional biopsy and cytology can have unacceptable false negative rates often arising from sampling errors. Therefore optical imaging techniques have gained popularity for medical diagnostics.

Time-domain optical imaging using short pulse lasers has developed as a powerful tool in medical diagnostics. This technique presents several advantages over other conventional cw imaging techniques. Short pulse laser probing techniques for diagnostics have distinct advantages over very large pulse width or continuous wave lasers primarily due to the additional information conveyed by the temporal distribution of the observed signal.[1,2,3,4] The distinct feature is the multiple scattering induced temporal distributions, which persists for a time period greater than the duration of the source pulse and is a function of the source pulse width as well as the optical properties of the medium. If the detection is carried out at the same short time scale (comparable to the order of the pulse width), the signal continues to be observed even at large times after the pulse has been off due to the time taken for the photons to migrate to the detector

* kmitra@fit.edu; 150 W. University Blvd., Melbourne, FL 32901; phone: (321) 674 7131; fax: (321) 674 8813
** vodinht@ornl.gov; P.O. Box 2008, M.S. 6101, Oak Ridge, TN 37831-6101; phone: (865) 574 6249; fax: (865) 576 7651

Advanced Biomedical and Clinical Diagnostic Systems IV,
edited by Gerald E. Cohn, Warren S. Grundfest, David A. Benaron, Tuan Vo-Dinh,
Proc. of SPIE Vol. 6080, 608005, (2006) · 1605-7422/06/$15 · doi: 10.1117/12.664121

after multiple scattering in the media. Therefore detectors with high temporal resolution are required to collect the scattered reflected and transmitted photons.

Time-resolved techniques improve the localization and characterization of the inhomogeneities as information on the path length of each photon becomes available. Inhomogeneities differing from the surrounding tissue in terms of optical properties have different influence on the distribution of times of flight of photons. The temporal shape of the measured optical signals provides detailed information about medium characteristics including presence of inhomogeneities and tumors.

In order to predict the optical properties of tissues from time-resolved scattered optical signal measurements, development of inverse algorithm is required. Before development of complex inverse algorithms, accurate forward solutions of transient radiative transport equation necessary to analyze short-pulse laser propagation through tissues are critical. In most previous analysis, the transient term of the radiative transport equation (RTE) is usually neglected. The simulation of the transient radiation transport process is more complicated than the traditional steady-state analysis due to the hyperbolic wave nature of the equation coupled with the in-scattering integral term making it an integro-differential equation.[3,4] Diffusion approximation has been commonly used in literature for solving the transient RTE for analyzing short pulse laser propagation through tissue media.[3,5,6,7] But time-resolved experiments on tissues have shown that diffusion-based analyses are accurate for thick samples but fail to match experimental data for sample thickness comparable to the mean free path.[8] Monte Carlo simulation results are found to match the experimental measurements on tissue phantoms but diffusion theory failed to accurately predict the scattering coefficient.[9] A detailed discussion of the validity of the diffusion in bio-optical imaging is also provided in the literature and it has been pointed out that diffusion approximations has limitation that should not be ignored.[10] Only a few studies have been devoted to multi-dimensional problems such as diffusion based three-dimensional model[11] and for phantoms containing inhomogeneities such as using of time-of-flight measurements.[12] Among all the methods, DOM is computationally inexpensive and is memory efficient as compared to other numerical schemes. It offers the best compromise between accuracy and computational time. There is no restriction on the optical thickness and scattering albedo variations while using DOM. Most of these previous studies have not compared the numerical modeling results with experimental measurements.

In order to compare the experimental measurements with the numerical modeling results, there is a need to develop accurate solutions of transient radiative transport equation in two- and three-dimensional geometry. Very few studies have been reported in literature regarding validation of experimental measurements with that obtained from the numerical models. Besides the model validation of experimental measurements for most of the previous work has been primarily restricted to homogenous samples.[13,14,15] Moreover validation of experimental measurements for tissue phantoms containing inhomogeneities reported in the literature has been performed using diffusion based model.[2,16,17] Authors of this group have validated the experimental measurements of transmitted signals for tissue phantoms with inhomogeneities imbedded in them with solutions of RTE obtained using DOM.[18] More studies are necessary for validation of forward model of RTE with experimental measurements for determination of tissue optical properties. Moreover, the measurement of transmitted optical signals is not practical for imaging internal organs such as brain, lung, kidneys etc. for cancer / tumor detection. Hence there is a need for measurement and validation of both the reflected and transmitted scattered optical signals from tissue phantom containing inhomogeneities.

Small animal imaging systems have received increasing attention over the past decade. The interest is motivated by advances in animal models of human diseases and possibility to non-invasively monitor the progression of diseases in living small animals. Different imaging techniques such as confocal imaging,[19] single photon emission tomography,[20] MRI imaging,[21,22] fluorescence imaging,[23] cw optical tomography[22] have been used for the detection of tumors in small animals. However very few studies have been reported on time-domain optical imaging of animals. The goal of this paper will be to demonstrate the feasibility of using the time-resolved optical tomography system using short pulse laser for detection of tumors in rats.

A fiber optic system is used for the laser incidence as well as for the collection of scattered reflected and transmitted optical signals from the samples. The fiber optic probe assembly mounted on a 3-axis translation stage is used to scan any tissue area and is connected to a computerized data acquisition system. The measured optical signals from the scanned area are directly fed into National Instrument's LabView 7.1 software to view the 3-D distribution of the

intensity in real time. The advantages of using a fiber optic approach are the high transmission efficiency of fiber optics and the fact that light can easily transmitted to remote locations for imaging of internal organs inside the body.

In this paper first experimental measurements of both the scattered reflected and transmitted signals are validated with the numerical modeling results obtained by solving the RTE using DOM for tissue phantoms containing inhomogeneities. Experiments are next performed on freshly excised rat tissue samples and the measured reflected optical signal measurements are also validated with the numerical modeling results. To the authors' knowledge this would be the first time that experimental validation of the optical signal measurements using numerical models has been performed on animal tissue samples. Experiments are finally performed on anaesthetized rats with tumor-promoting agents applied on the skin to analyze their effect on optical signals. The goal is to demonstrate the feasibility of using time-resolved optical tomography system for detection of tumors in animal model.

2. THEORETICAL FORMULATION

In this paper the tissue medium is approximated by an anisotropically scattering and absorbing rectangular enclosure in which an inhomogeneity is imbedded (see Fig. 1). The transient radiative transfer equation is used to analyze short pulse laser propagation through tissues and is given by:[4,25]

$$\frac{1}{c}\frac{\partial I(x,y,\Omega,t)}{\partial t}+\mu\frac{\partial I(x,y,\Omega,t)}{\partial x}+\eta\frac{\partial I(x,y,\Omega,t)}{\partial y}+k_e I(x,y,\Omega,t)=\frac{k_s}{4\pi}\int_{4\pi}\Phi(\Omega',\Omega)I(x,y,\Omega',t)\,d\Omega'+S(x,y,\Omega,t) \quad , \quad (1)$$

where I is the scattered diffuse intensity ($Wm^{-2}sr^{-1}$), k_e and k_s are the extinction coefficient and the scattering coefficient respectively, Φ is the phase function, Ω is the solid angle, c is the velocity of light in the medium, x and y are the spatial coordinates, t is the time and S is the source term. The pulsed radiation incident on the tissue medium (see Fig. 1) is a Gaussian pulse having a temporal duration (pulse width) t_p at full width half-maximum (FWHM). The total intensity can be separated into a collimated component, corresponding to the incident source pulse and a scattered intensity I as described by Eq. (1). The source function S in Eq. (1) is due to the collimated component of the irradiation.

Numerical results have been obtained by solving the above transient radiative transfer equation using discrete ordinate method as described in details in previous papers of the authors[25,26] and is not repeated here. The computational time is about 180 seconds on a LINUX Workstation with a 3.2 GHz CPU for 80 discrete ordinates quadratures. Spatial grid size of 0.5 mm and temporal grid size of 0.5 ps is used in the simulations. The accuracy of the numerical results is validated by ensuring the results are independent of the grid sizes. The sample height is very large compared to the beam diameter and hence a two-dimensional transient radiative transfer model is applied. Results obtained using numerical simulations are compared with the corresponding reflected and transmitted optical signals measured experimentally.

3. EXPERIMENTAL METHODS

The schematic of the experimental setup for measurement of scattered reflected optical signals for the case of imaging of rats with mammary tumor is shown in Fig. 2. The schematic of the setup for measurements of the transmitted optical signal is not presented here and can be found in the literature.[18]

The laser beam is first incident on a plate type beam splitter. The first beam splitter divides the emitted laser beam into two parts in the ratio of 9:1. The part having 10% of the main laser beam is passed though a delay generating prism and fed into the Hamamatsu streak camera unit (C 1587) for observing the raw pulse as a reference. A second beam splitter further splits the beam with 90% of main laser beam energy into two parts again in the ratio of 9:1. The beam with 90% energy of the split beam is focused onto the excitation end of a fiber optic probe and is then transmitted to the distal end where it illuminates the samples. The beam with 10% energy of the split beam is further split by a third beam splitter in the ratio of 9:1. The beam with 90% energy of the split beam is used to monitor the pulse width of the incident beam using an 18.5 ps ultra fast photo-detector (New-focus, Model 1954). The output of the detector is measured on the Tektronix (7854) oscilloscope with sampling modules. The beam with 10% of the energy of the split beam is used to monitor the power of the laser beam incident on the sample using appropriate calibration.

To feed the laser light into the fibers for precise and efficient delivery of light to the samples, various focusing elements such as lenses, mirrors and collimators are used. The scattered reflected and transmitted optical signals from the samples collected using the fiber optic probe is fed into the same Hamamatsu streak camera. The probe assembly is mounted on a 3-axis vertical translation stage. The average power incident on the sample is of the order of 12-15 mW. Hence attenuators are used to reduce the incident power on the samples as required so as not to saturate the streak camera. The fiber used in the study is a 1 m long multimode fiber with a core diameter of 62.4 μm and outer diameter of 125μm, a numerical aperture of 0.21 and V number of 222.314. The beam attenuation inside the fiber is 5 dB/km. The fibers have FC connectors at both ends. The typical insertion loss of the FC connector is around 0.3 dB.

Typical tissue phantom used in this study as shown in Fig. 1 have dimensions of 50 mm (width, W) x 25 mm (height, H) x 8 mm (thickness, L). The tissue phantoms are made of Araldite 502 embedding medium. Araldite 502 resin is polymerized with Dodecenyl Succinic Anhydride (DDSA) and catalyzed with 2,4,6-Tri Phenol (DMP-30) in the volumetric ratio of 1: 0.85: 0.04. Titanium Dioxide (TiO_2) having mean diameter = 0.3 μm is added as scatterers to the resin base and India Ink is used as absorber. Details about phantom preparation can be obtained from literature.[18] Inhomogeneities typically of 4 mm diameter are drilled in the center of the samples and filled with material having different optical parameters compared to the base tissue matrix.

Freshly excised rat tissue samples are obtained from Wistar Rat of Alvino trait. Tissue samples are cut in such a way that either skin or skin and muscle combined are obtained to study the effect of different layers. The rat skin layers are typically 3 mm thick while the tissue samples with combined skin and muscle layers are typically 8 mm thick. Typical cross-section of the tissue samples used are 30 mm x 20 mm.

Experiments are next performed on anaesthetized rat with tumor-promoting agents injected on the skin surface and as well as below the skin surface. Studies are performed on rats which are anesthetized with ketamine hydrochloride (Ketaset, Ft. Dodge Laboratories, Ft. Dodge, IA, USA), administered IP at 150mg/kg. The tumor diameter is around 2 mm. After the completion of the experiments, rats are allowed to recover from the effects of anesthesia before being introduced to the animal colony.

4. RESULTS

Experiments are first performed on homogeneous tissue phantoms and tissue phantom containing inhomogeneities to optimize the time-resolved optical tomography system. Scattered optical reflected and transmitted signal measurements are validated with the numerical modeling results. Next experiments are performed on *in vitro* tissue samples to characterize the optical signatures from real tissues and compare the experimental measurements with the numerical modeling results. Finally *in vivo* experiments are performed in live anaesthetized rats with tumor-promoting agents applied on the skin surface and injected below the skin surface and as well as in live anaesthetized mouse with mammary tumors to demonstrate the feasibility of using this technique for tumor detection in animal model.

In Fig. 3 the normalized transmitted signals are compared between a homogenous tissue phantom and that of a phantom containing inhomogeneity at the center having different scattering coefficients. For the homogenous tissue phantom the values of scattering coefficient (k_s) and absorption coefficient (k_a) used are 10 mm^{-1} and 0.05 mm^{-1} respectively.[27] The thickness (L) of the tissue phantoms for all the cases is 8 mm. For the tissue phantom containing inhomogeneity the optical properties of the base tissue phantom is same as that of the homogenous phantom while two different values of scattering coefficients of the inhomogeneity (k_{si}) are used: 20 mm^{-1} and 40 mm^{-1}. The absorption coefficient of the inhomogeneity (k_{ai}) is kept the same as base tissue matrix and is equal to 0.005 mm^{-1}. There is a very good agreement between numerical modeling results and experimental measurements with a little separation in the tail section. This separation can be attributed to the fact that as scattering coefficient is increased the photons suffer random scattering and persist inside the medium for a longer time resulting in very few photons leaving the medium and thus contributing to the noise. Further, normalization of signal also amplifies the noise at the tail of the pulse. It is observed that with the increase in the scattering coefficient of the inhomogeneity, the temporal broadening of the output transmitted pulse (t_{bp}) increases. Higher scattering coefficient increases the optical depth of the medium and as a result the transmitted photons take a longer time to reach the detector which is manifested in the higher temporal broadening of the transmitted optical signal. Figure 4 shows the comparison of the normalized reflected signals between a homogenous tissue phantom and the tissue phantom containing inhomoegneity at the center for different absorption coefficients of the inhomogeneity.

The scattering coefficient of the inhomogeneity is kept constant at 20 mm^{-1} while two different values of absorption coefficients of the inhomogeneities are used: 0.5 and 0.005 mm^{-1}. With the increase in the absorption coefficient of the inhomogeneity greater number of photons is absorbed within the medium. This results in greater attenuation of the incident light and as a result the total temporal broadening of the reflected pulse reduces with increase in the absorption coefficient. For both Fig. 3 and Fig. 4 there is also a change in the magnitude of the intensity values but this effect is masked due to the normalization of the signals.

Figure 5 shows the comparison between numerical modeling results and experimentally measured transmitted and reflected signals for the best time instant of 325 ps. In time resolved optical tomography, the contrast of the image is a strong function of time instant chosen. Hence the choice of time instant providing best contrast (325 ps for this case) is a very important parameter. In Fig. 5 a very good match is observed between the experimental measurements and the numerical modeling results. The transmitted and reflected signals show an opposite trend. While the reflected intensity is highest at the location of the inhomogeneity, the transmitted intensity is lowest at that location. This is because, since the inhomogeneity has higher scattering coefficient compared to the surrounding base tissue, a larger number of incident photons gets scattered and comes back to the detector compared to that from homogeneous base tissue region during reflection measurement. Hence the spatial reflected signal shows a peak at the inhomogeneity location. On the other hand, as large number of photons gets scattered, only few photons penetrate the phantom thickness and reaches the detector during transmission measurement compared to that from base tissue region. This results in a deep trough in spatial profile of transmitted signal at the inhomogeneity site.

Analysis of laser-tissue interaction characteristics is necessary to obtain information about variation of tissue optical properties with depth. Variation of tissue optical properties in different tissue layers can be used to monitor progression of diseases by measuring the signal origin and intensity. Therefore, as a first step it is necessary to analyze laser interaction with healthy tissue layers to calibrate the system parameters. Tissue can be modeled primarily as having two main layers: epithelium composed of several layers of epithelial cells and stroma consisting mostly of extracellular matrix proteins and blood vessels. Therefore, once the time-resolved optical detection scheme has been optimized with experiments on tissue phantoms, *in vitro* experiments are next performed on freshly excised rat tissue samples to characterize the optical signatures from these samples. Temporal optical signatures from rat skin and muscle samples are compared with the numerical modeling results. Figure 6 shows the normalized reflected signals for freshly excised rat skin sample and as well rat skin and muscle combined sample. The optical properties of rat skin and muscle are obtained from the literature.[27,28] Skin and muscle combined sample is thicker as compared to skin only sample. As a result the photons encounter more multiple scattering reaching the detector while traveling through combined skin and muscle sample than through skin sample. This result in higher temporal broadening of the reflected optical signals from skin and muscle combined compared to that from skin only sample for the same incident power. The random scattering inside muscle causes diffuse spreading of light over a large volume. Greater optical thickness also results in greater attenuation of the incident light.

The next step is to conduct experiments on anaesthetized rats with tumor-promoting agents applied on the skin surface as well as injected below the skin surface. For the case of tumor-promoting agents injected below the skin surface, the depth of the tumor from the surface is unknown and the goal is to detect the exact location and depth of the tumor from the surface using time-resolved measurement techniques. Schematic of the rat with tumor location is shown in Fig. 7. Figure 8 gives us a quantitative idea about the depth at which the tumor is located below the skin surface. It is observed from Fig. 8 that the reflected intensity has highest magnitude for rat with no tumor-promoting agent injected since the tumor has higher absorption than the healthy tissue. Therefore the reflected signal is significantly attenuated for the case of tumor-promoting agent applied on the skin surface and injected below the skin surface. The key feature in this figure is the peak separation of 15 ps between the reflected signals from the tumor located below the skin and from the tumor located on the skin surface. 15 ps is the additional time taken by the reflected photons from the tumor on the surface to reach the detector compared to the photons reflected from the tumor located below the skin surface. With the tumor-promoting agent on the skin surface, majority of the photons are absorbed and very few are reflected while for tumor-promoting materials injected below the skin surface more photons are reflected from the skin surface and relatively few photons reach the tumor location. Multiplying the peak separation time between the reflected signals for the two cases by the speed of light in tissues (3×10^8 m/s / 1.54 = 1.95×10^8 m/s) gives the depth of the tumor as 15 ps × 1.95×10^8 m/s = 2.95 mm. Thus using this technique a quantitative idea about the depth at which tumors are located below the skin surface can be obtained. The exact size of the tumor and also the tumor location can be obtained from the spatial profiles

of the reflected optical signals by scanning over a length AB as shown in Fig. 7. Figure 9 shows the spatial profiles of the reflected intensity at a particular time for tumor-promoting agents applied to the surface and as well as injected below the surface of the skin. It is observed that the reflected signals have the lowest intensity magnitude at the location of the tumor while it increases away from the tumor site. Since tumor have higher absorption coefficient due to increased blood supply it results in more absorption of photons at the tumor site compared to the surrounding healthy tissue. Therefore a reduction of the reflected intensity magnitude is observed at the tumor location.

5. CONCLUSIONS

In this work an extensive analysis has been performed to investigate the interaction of light with tissues with the goal of tumor detection. The experimental measurements for the case of various types of tissue phantoms and freshly excised tissue samples are in excellent agreement with the numerical modeling results. By the parametric variation of the scattering and absorption properties of the embedded inhomogeneity inside the tissue phantom, it is possible to characterize the propagation of light under various structural and physiological conditions of tissues and extract pertinent information about them. Temporal profiles of the optical signals help in providing information about the tissue optical properties while the spatial profile at a particular time window helps in locating the tumor/inhomogeneity location. In time-resolved detection technique the selection of appropriate time window is critical for identifying the inhomogeneity embedded inside the tissue medium. It is observed from the time-resolved optical signal measurements in rats that one can predict the precise size, location of the tumor, and also the depth at which the tumor is located below the skin surface.

ACKNOWLEDGEMENTS

Kunal Mitra acknowledges partial support from Oak Ridge National Laboratory through Contract No. 4000004751. Tuan Vo-Dinh acknowledges support from NIH grant No. 1 R01 CA88787-01 and US Department of Energy, Office of Environmental and Biological Research under Contract No. DE-AC05-00OR22725 with UT Battelle, LLC.

REFERENCES

1. F. Liu, K. M. Yoo, and R. R. Alfano, "Ultrafast laser-pulse transmission and imaging through biological tissue," *Appl. Opt*. **32**, 554-558 (1993).
2. S. Proskurin, Y. Yamada, and Y. Takahashi, "Absorption coefficient measurements of strongly scattering media using time-resolved transmittance of a short pulse in near-infrared wavelength range," *Opt. Rev.* **2**, 292-297 (1995).
3. Y. Yamada, "Light-tissue interaction and optical imaging in biomedicine," *Ann. Rev. Fluid Mech. Heat Transfer* **6**, 1-59 (1995).
4. S. Kumar, K. Mitra, and Y. Yamada, "Hyperbolic damped-wave models for transient light-pulse propagation in scattering media," *Appl. Opt*. **35**, 3372-3378 (1996).
5. R. Berg, S. Andersson-Engels, O. Jarlman, and S. Svanberg, "Time-gated viewing studies on tissue-like phantoms," *Appl. Opt.* **35**, 3432-3440 (1996).
6. M. S. Patterson, B. Chance, and B C. Wilson, "Time resolved reflectance and transmittance for the non-invasive measurement of tissue optical properties," *Appl. Opt.* **28**, 2331-2336 (1989).
7. A. Ishimaru, Y. Kuga, R. L. T. Cheung, and K. Shimizu, "Scattering and diffusion of a beam wave in randomly distributed scatterers," *J. Opt. Soc. Am.* **73**, 131-136 (1983).
8. K. M. Yoo, F. Liu, and R. R. Alfano, "When does the diffusion approximation fail to describe the photon transport in random media," *Phys. Rev. Lett.* **65**, 2647-2650 (1990).
9. A. H. Heelscher, S L. Jacques, L. Wang, and F. K. Tittel, "Influence of boundary conditions on the accuracy of diffusion theory in time-resolved reflectance spectroscopy of biological tissues," *Phys. Med. Biol.* **40**, 1957-1975 (1995).
10. B. Chen, K. Stamnes, and J. J. Stamnes, "Validity of the diffusion approximation in bio-optical imaging," *Appl. Opt.* **40**, 6356-6366 (2001).
11. S. Arride, J. Hebden, M. Schweiger, F. Schmidt, M. Fry, E. Hillman, H. Dehghani, and D. T. Delpy, "A method for three-dimensional time-resolved optical tomography," *Int. J. Imag. Sys. Tech*. **11**, 2-11 (2000).
12. A. Gandjbakhche, V. Chernomordik, J. C. Hebden, and R. Nossal, "Time-dependent contrast functions for quantitative imaging in time-resolved transillumination experiments," *Appl. Opt.* **37**, 1973-1981 (1998).

13. M. Q. Brewster, and Y. Yamada, "Optical properties of thick, turbid media from picosecond time-resolved light scattering measurements," *Int. J. Heat Mass Trans.* **38**, 2569-2581 (1995).
14. J. M. Tualle, E. Tinet, and S. Avrillier, "New and easy way to perform time-resolved measurements of the light scattered by a turbid medium," *Opt. Comm.* **189**, 211-220 (2001).
15. Z. Guo, J. Aber, B. A. Garetz, and S. Kumar, "Monte Carlo simulation and experiments of pulsed radiative transfer," *J. Quant. Spect. Rad. Transf.* **73**, 159-168 (2002).
16. D. J. Hall, J. C. Hebden, and D. T. Deply, "Imaging very-low-contrast objects in breast-like scattering media with a time-resolved method," *Appl. Opt.* **36**, 7270-7276 (1997).
17. R. Cubeddu, A. Pifferi, P. Taroni, A. Torricelli, and G. Valentini, "Imaging of optical inhomogeneities in highly diffusive media: Discrimination between scattering and absorption contribution," *Appl. Phys. Lett.* **69**, 4162-4164 (1996).
18. C. Das, A. Trivedi, K. Mitra, and T. Vo-Dinh, "Experimental and numerical analysis of short-pulse laser interaction with tissue phantoms containing inhomogeneities," *Appl. Opt.* **42**, 5173-5180 (2003).
19. A. A. Lacy, T. Collier, J. E. Price, S. Dharmawardhane, R. Richards-Kortum, "Near real-time *in vivo* confocal imaging of mouse mammary tumors," *Front. Biosci.* **7**, 137-145 (2002).
20. P. D. Acton, and H. F. Kung, "Small animal imaging with high resolution single photon emission tomography," *Nuc. Med. Biol.* **30**, 889-895 (2003).
21. M. R. Rajeswari, A. Jain, A. Sharma, D. Singh, N. R. Jagannathan, U. Sharma, and M. N. Degaonkar, "Evaluation of skin tumors by magnetic resonance imaging," *Lab. Invest.* **83**, 1279-1283 (2003).
22. J. Masciotti, G. Abdoulaev, J. Hur, J. Papa, J. Bae, J. Huang, D. Yamashiro, J. Kandel, and A. H. Hielscher, "Combined optical tomographic and magnetic resonance imaging of tumor bearing mice," *Proc. SPIE* **5693**, 74-81 (2005).
23. N. Ramanujam, J. Chen, K. Gossage, R. Richards-Kortum, and B. Chance, "Fast and noninvasive fluorescence imaging of biologic tissues i*n vivo* using a flying-spot scanner," *IEEE Trans. Biomed. Eng.* **48**, 1034-1041 (2001).
24. M. Firbank, D. T. Delpy, "Design for a stable and reproducible phantom for use in near infra-red imaging and spectroscopy," *Phys. Med. Biol.* **38**, 847 (1993).
25. K. Mitra, and S. Kumar, "Development and comparison of models for light pulse transport through scattering absorbing media," *Appl. Opt.* **38**, 188-196 (1999).
26. M. Sakami, K. Mitra, and P. Hsu, "Analysis of light-pulse transport through two-dimensional scattering-absorbing media," J. Quant. Spect. Rad. Transf. **73**, 169-179 (2002).
27. W. F. Cheong, S. A. Prahl, and A. J. Welch, "A review of the optical properties of biological tissues," *IEEE J. Quant. Electron.* **26**, 2166-2185 (1990).
28. A. M. K. Nilsson, R. Berg, and S. Andersson-Engels, "Measurements of optical properties of tissue in conjunction with photodynamic therapy," *Appl. Opt.* **34**, 4609-4619 (1995).

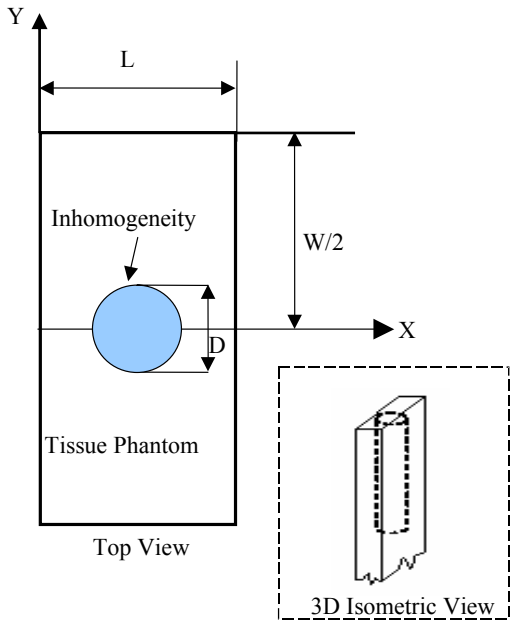

Figure 1. Schematic of the phantom containing inhomogeneity.

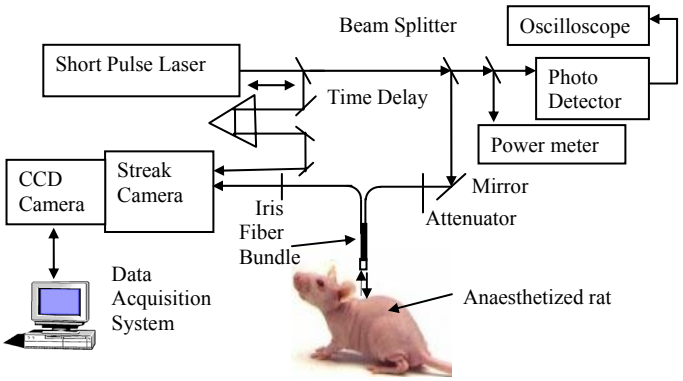

Figure 2. Schematic of the experimental setup.

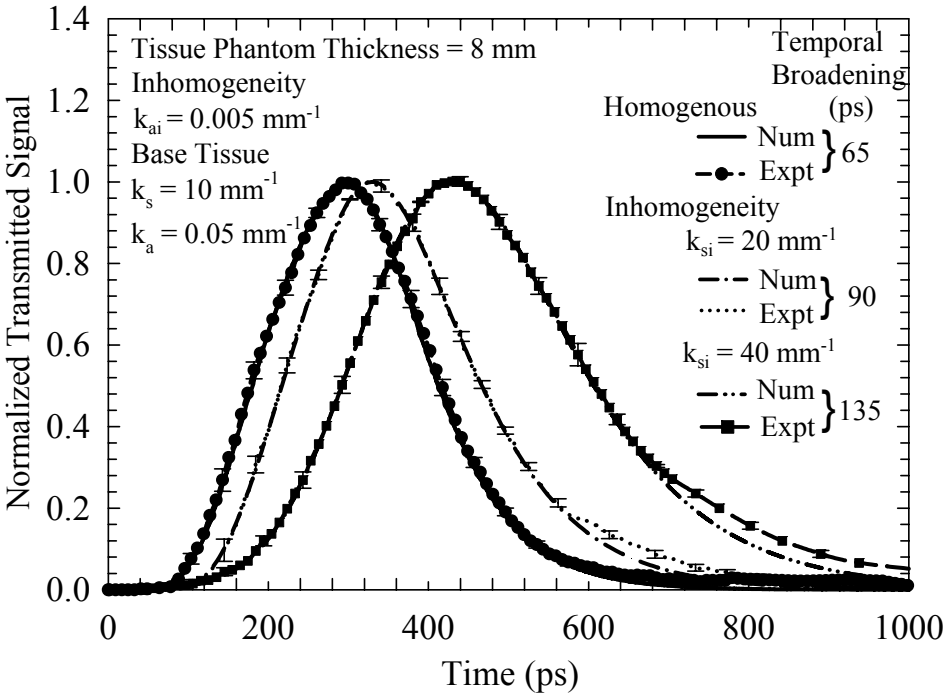

Figure 3. Effect of variation of scattering coefficient of embedded inhomogeneity on temporal transmitted signals for tissue phantoms containing inhomogeneity.

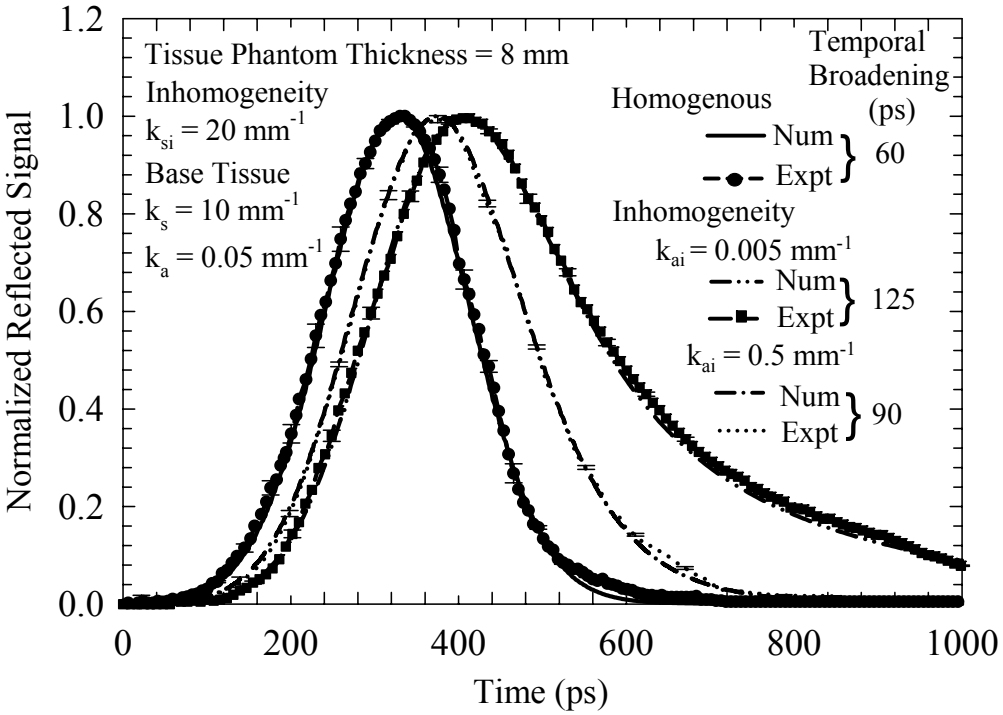

Figure 4. Effect of variation of absorption coefficient of embedded inhomogeneity on temporal reflected signals for tissue phantoms containing inhomogeneity.

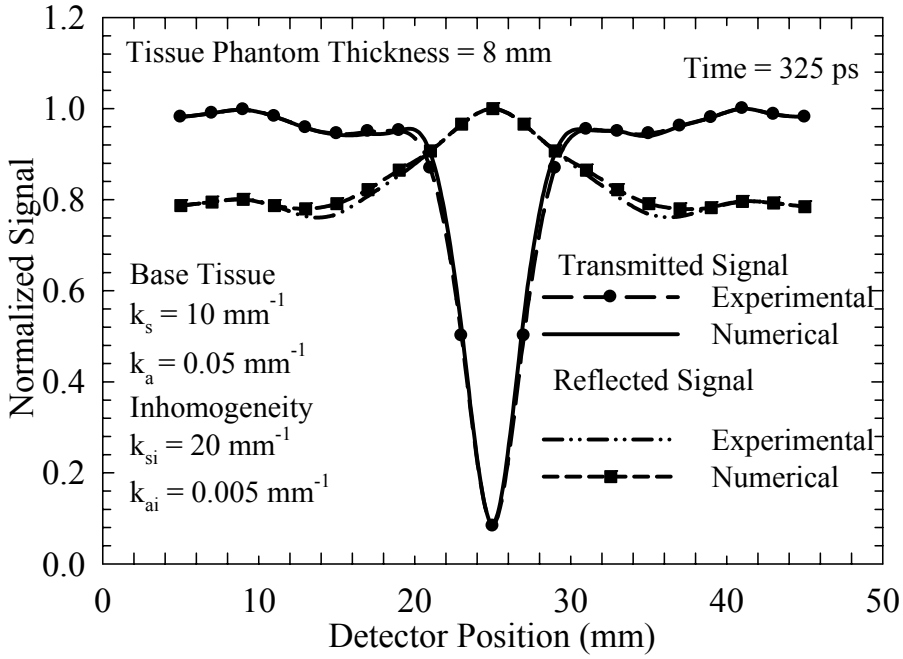

Figure 5. Spatial transmitted and reflected signals for a tissue phantom containing inhomogeneity at the time instant with best contrast.

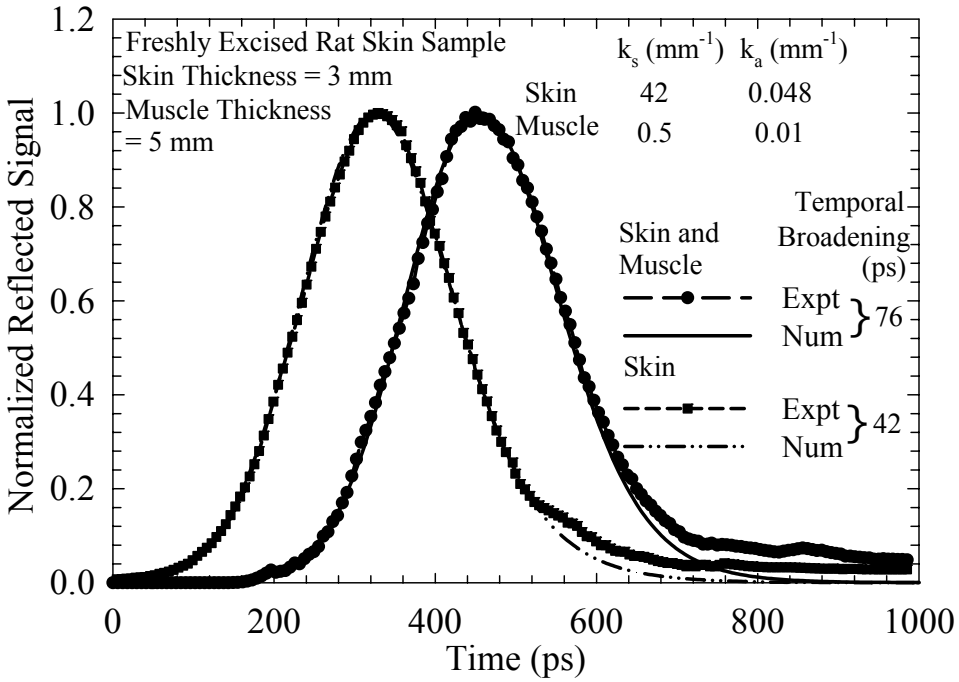

Figure 6. Temporal reflected signals for freshly excised rat tissue samples.

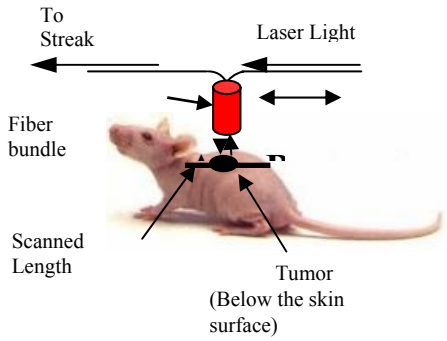

Figure 7. Schematic of scanning location of anaesthetized rat injected with tumor-promoting agent.

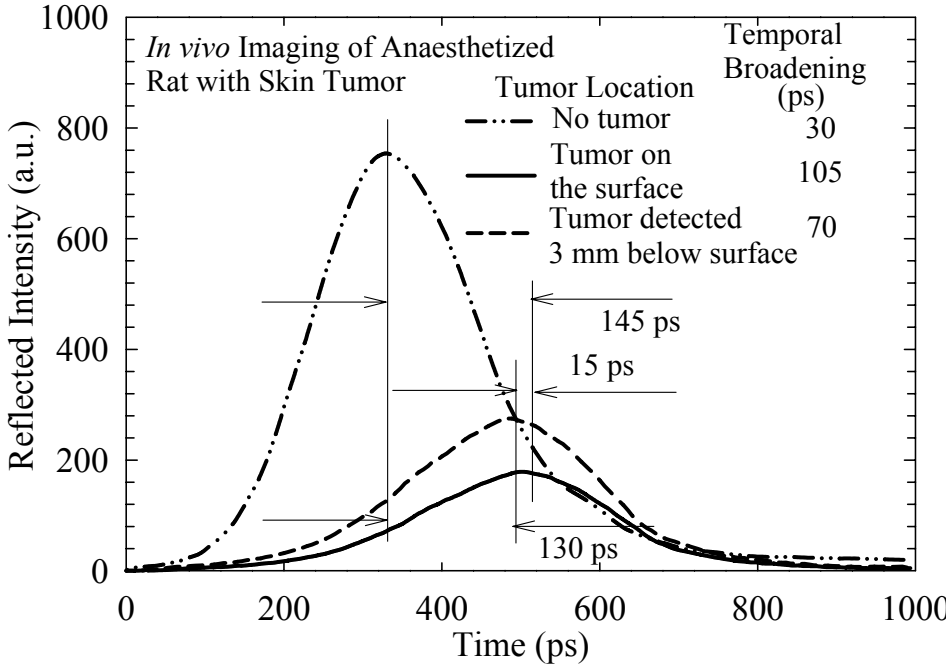

Fig. 8. Temporal reflected intensities for different tumor locations in anaesthetized rat.

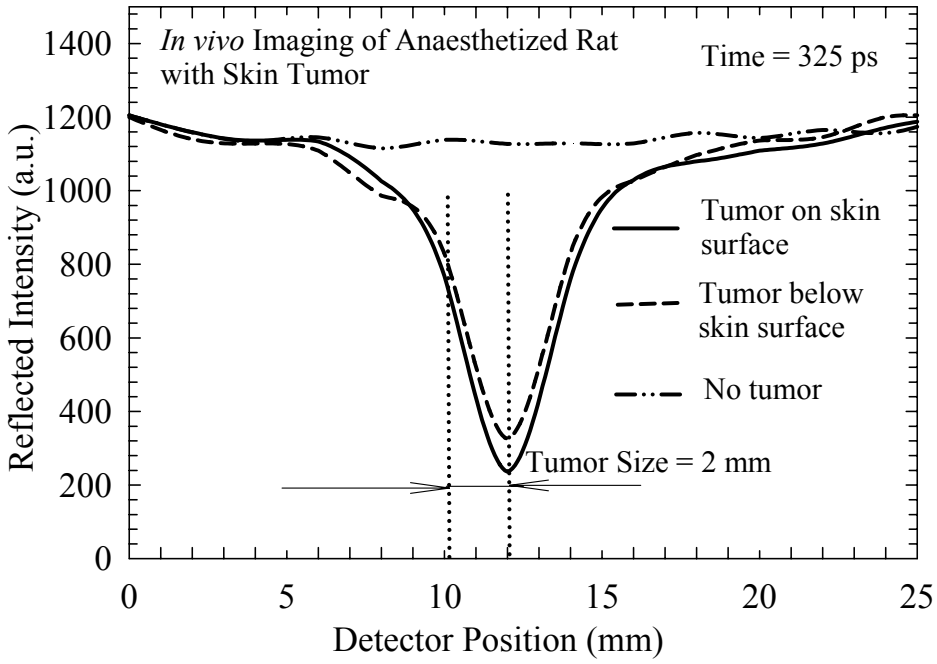

Fig. 9. Spatial reflected intensities for different tumor locations in anaesthetized rat.